

Investigation on utilization of liquid propellant in ballistic range experiments

Akihiro SASOH*, Shinji OHBA**, and Kazuyoshi TAKAYAMA***

Experiments were conducted in a ballistic range using a HAN (hydroxylammonium nitrate)-based liquid monopropellant, LP1846. In a 25-mm-bore single-stage gun, using bulk-loaded propellant of 10 to 35g, a muzzle speed up to 1.0km/s was obtained. Time variations of propellant chamber pressures and in-tube projectile velocity profiles were measured. The liquid propellant combustion was initiated accompanying a delay time which was created due to the pyrolysis of the propellant. In order to obtain reliable ballistic range performance, the method of propellant loading was revealed to be critical. Since the burning rate of the liquid propellant is relatively low, the peak acceleration and the muzzle speed strongly depend on the rupture pressure of a diaphragm that was inserted between the launch tube and the propellant chamber.

1. Introduction

A ballistic range serves various purposes such as a hypersonic ground test facility, a hypervelocity impact test and a drug delivery system. Related technologies are extended to many industrial, engineering and even medical systems. Required performance of a ballistic range depends solely on the condition of applications. In particular, in order to launch a fragile model, the ballistic range design requires a low level

of peak acceleration. The development of a device which has such a characteristic definitely warrants further intensive studies. For example, in the ram accelerator installed at the Shock Wave Research Center¹⁾, a 35 gram projectile which has a complicated geometry and a sabot the perforation ratio of which is of the order of 50% have to be pre-accelerated up to 1.15 km/s currently by using smokeless powder. With limited facility resources, this required performance is not readily achieved and still necessitates further improvement of the pre-acceleration device.

Liquid propellants has been studied as an alternative propellant to solid propellants for tactical applications mainly in Europe and U.S.A. Excellent summaries of the previous works are described in Refs. 2 and 3. In addition to some practical advantages, under an appropriate operation condition liquid propellants are known to have a favorable characteristic of a flat pressure-time profile. By utilizing this, smooth acceleration of a fragile projectile with a high piezometric efficiency (the ratio of the mean pressure to the peak breech pressure, p.29 in Ref. 2) would be potentially achievable. A high piezometric efficiency implies that a high thrust is kept down to the muzzle with a peak mechanical load being suppressed low,

Received on April 13, 1999

*Shock Wave Research Center
 Institute of Fluid Science, Tohoku University
 2-1-1 Katahira, Aoba-ku, Sendai 980-8577, JAPAN
 TEL +81-22-217-5284
 FAX +81-22-217-5284
 e-mail sasoh@ifs.tohoku.ac.jp

**Graduate School, Department of Aeronautics and Space Engineering, Tohoku University currently, JGC Co.
 5th fl. Shin-Ohtemachi Bldg. Ohtemachi, Chiyoda-ku, Tokyo 100-0004, JANAN
 TEL +81-3-3279-5441
 FAX + 81-3-3273-8047

***Shock Wave Research Center
 Institute of Fluid Science, Tohoku University
 2-1-1 Katahira, Aoba-ku, Sendai 980-8577, JAPAN
 TEL +81-22-217-5283
 FAX +81-22-217-5324
 e-mail takayama@ifs.tohoku.ac.jp

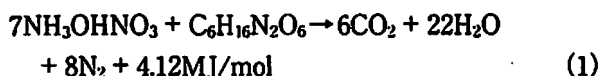
and the projectile is efficiently accelerated

Among various liquid propellants, HAN (hydroxylammonium nitrate; $\text{NH}_2\text{OH} \cdot \text{HNO}_3$)-based mono-propellants have low toxicity and sensitivity, and are most widely used. Their combustion characteristics and related fundamental investigation were conducted also in Japan⁴⁻⁶⁾. Recently, this type of propellant once again attracts an attention as a candidate of rocket propellant⁷⁾.

The purpose of this paper is to basically study ballistic range characteristics of a typical liquid propellant, LP1846, and to examine the applicability of the propellant to laboratory experiments.

2. Properties of LP 1846

LP1846 is a mixture of HAN, TEAN (trietanolammonium nitrate; $\text{C}_6\text{H}_{16}\text{N}_2\text{O}_6$) and water. Their molar ratio is HAN : TEAN : H_2O = 7 : 1 : 12.3²⁾. In the propellant, TEAN takes a role as a fuel. HAN acts as an oxidizer. Their reaction formula is



Therefore, the equivalence ratio of LP 1846 is unity. The above stoichiometric combustion yields the non-toxic products. Accounting the water contents, the average molecular mass of the product is 22.9 kg/kmol. The impetus (or force) of the propellant is 0.899MJ/kg²⁾.

3. Experimental apparatus

Fig. 1 shows a schematic illustration of the single-stage gun of the Shock Wave Research Center, Institute of Fluid Science, Tohoku University. Its launch tube has an inner diameter of 25 mm and a length of 2.0m, and is connected into a test chamber. The initial pressure in the test chamber was lower than 100Pa. The test chamber has a pair of 300-mm-dia.

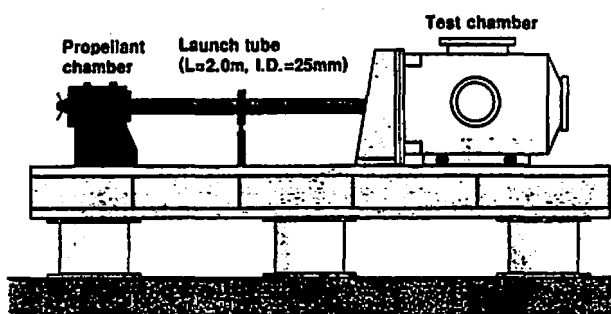


Fig. 1 Single-stage gun

acrylic windows, through which two diode laser beams were set to measure the muzzle speed by means of the method of time of flight. Also through the window, an argon-ion laser beam and its reflected beam pass for measuring an in-bore projectile velocity by using a VISAR (Velocity Interferometer System for Any Reflector). For detailed description of the VISAR measurement, the readers should refer to other articles⁹⁻¹¹⁾.

The propellant chamber, Fig. 2, configures almost as a cylinder. It has an inner diameter of 35mm and a length of 113mm. At its outlet end, a layer of metal diaphragm is inserted. The static rupture pressure is controlled by varying the material and thickness of the diaphragm and the depth of the pressed groove on a surface of the diaphragm. In this study, the rupture pressure varied from 10 to 40MPa. The time variation of pressures in the propellant chamber were measured using piezo-electric pressure transducers. The pressure transducers, P1 and P2, were recess-mounted from the propellant chamber inner wall. The distance from the diaphragm to P1 is 80mm, that to P2 is 30 mm. The liquid propellant was bulk loaded. The ignition of the liquid propellant was assisted by using 0.9-gram smokeless powder (SS, Nippon Oil and Fat Co.), which, in turn, was ignited by an electrical ignitor.

Fig. 3 shows the design of the projectile under study. It is made of high-density polyethylene. It has a Bridgman seal on the base. The outer diameter around the Bridgman seal is slightly larger than the inner diameter of the launch tube. Except for this portion, its diameter is smaller than the launch tube

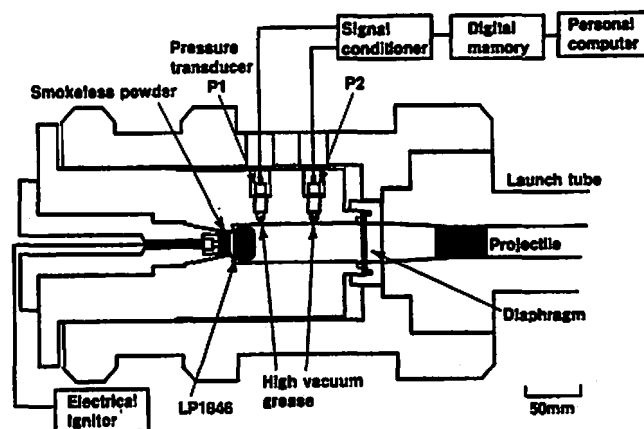


Fig. 2 Propellant chamber

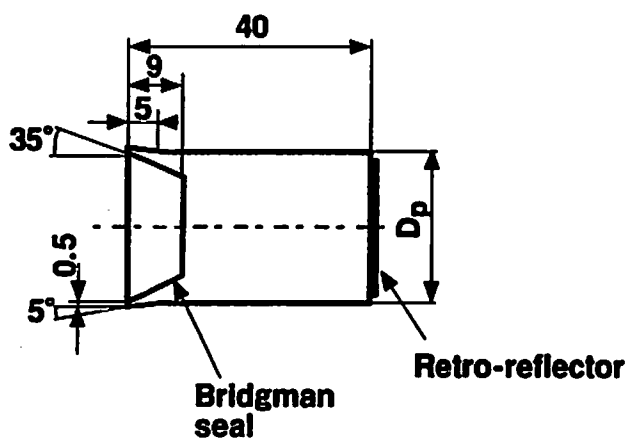


Fig. 3 Design of projectile

inner diameter by 0.28%. The total length of the projectile is 40mm. Its mass was 16.1 ± 0.08 g. On its frontal face, a layer of retro-reflective sheet (3970G, 3M) is attached. This sheet has a function that an incident laser beam is reflected in the exactly same direction as to the incident beam. This function is convenient for the in-bore velocity measurement using the VISAR.

4. Results and discussion

4.1 Basic propellant chamber pressure characteristics

Fig.4a and 4b show typical time variations of the propellant chamber pressures. The origin of the abscissa, t , designates the beginning of the data recording. In this paper, p_1 and p_2 designate measured pressures by P1 and P2 in Fig. 2, respectively. Note here that P1 is located at 80mm upstream from the diaphragm, and P2 is 30mm from it. Fig. 4a shows the whole recorded data of p_1 and Fig. 4b shows a blow-up of p_1 and p_2 variations around the moment of the diaphragm rupture. In Fig. 4a, events so far interpreted are marked by numbers. p_1 begins to rise at (1) and slowly increases during (2). The pressure rise during this period corresponds to burning of the smokeless powder. At the time zone (3), the propellant chamber pressure keeps an almost constant value. This delay in pressure rise for the main combustion is caused by the pyrolysis of the liquid propellant. Detailed discussion on this will be made in the following paragraphs and the next subsection. During the time zone (4), the main combustion of the liquid propellant takes place and the pressure sharply rises. At (5), the pressure suddenly drops because expansion waves caused by the rupture of the diaphragm arrives at the location of the

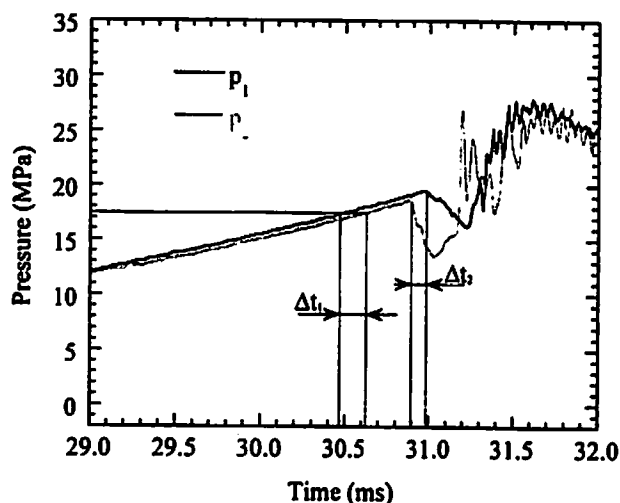
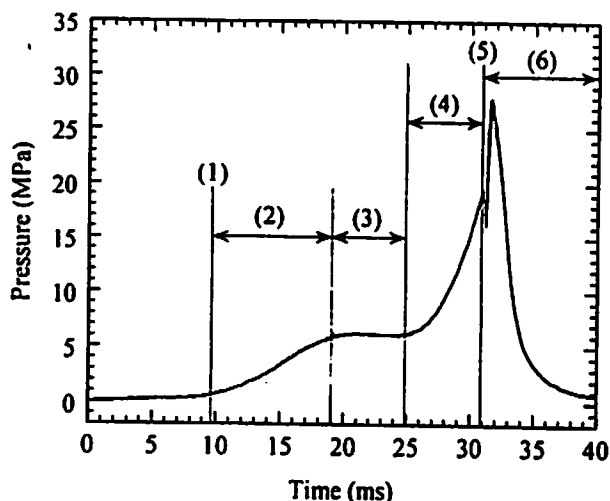


Fig. 4 Typical time variations of propellant chamber pressure. LP ; 30g, static diaphragm rupture pressure (p_r); 20 ± 33 MPa. (a) p_1 , (b) p_1 and p_2 around diaphragm rupture moment in shorter time scale

pressure transducer. It depends on the propellant burning rate and the motion of the projectile whether or not the pressure continues to increase even after the diaphragm rupture. In Fig. 4, it still increases after the diaphragm rupture. In the time zone (6), the projectile moves in the acceleration tube and the pressure decreases mainly due to the expansion of the product gas.

The characteristics of p_1 and p_2 appear to be vary similar. However, in a shorter time scale, those slightly differ. As seen in Fig. 4b, before the diaphragm rupture, there is a delay time, Δt_1 , for the pressure value of p_2 reaches the same value of p_1 . This implies that the combustion of the liquid propellant starts mainly near the ignitor. Compression waves generated due to its delayed combustion propagates

towards the muzzle. On the other hand, a pressure decrease caused by the diaphragm rupture appears to take place earlier in p_2 by Δt_2 . Those differences appeared well reproducibly in the present study. However, in a longer time scale during which projectile acceleration characteristics are discussed, such differences have only a subtle significance. Therefore, in the following discussions only p_1 profile will be presented.

In Fig. 5, the time variations of p_1 with and without the liquid propellant (LP) are compared with each other. Without the liquid propellant, the pressure is increased only by the combustion of the smokeless powder, so that p_1 begins to rise at $t = 4\text{ms}$, reaches its maximum at $t = 21\text{ms}$, and gradually decreases due to heat loss.

With the liquid propellant, the pressure rise profile at the early stage is similar. However, the peak pressure is slightly lower. It is believed that pyrolysis of the liquid propellant takes place during this period, thereby decreasing the propellant chamber pressure due to necessary heat for the pyrolysis. At a time interval from $t = 20\text{ms}$ to 26ms , p_2 remains an almost constant value, and then starts to increase due to the combustion of the liquid propellant.

4.2 Effects of liquid propellant loading

It was found that the ignition, combustion and acceleration characteristics were much affected by method of loading the liquid propellant. The liquid propellant was absorbed by a small piece of cotton, put into a bag made of $20\text{-}\mu\text{m}$ -thick polyethylene

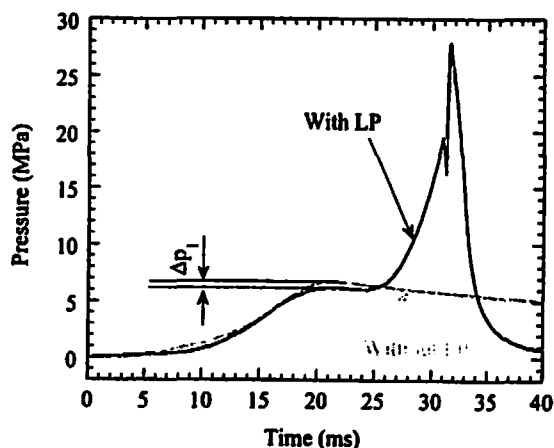


Fig. 5 Time variations of propellant chamber pressure, p_1 , with/without liquid propellant. p_1 with LP is the same as of Fig. 4a

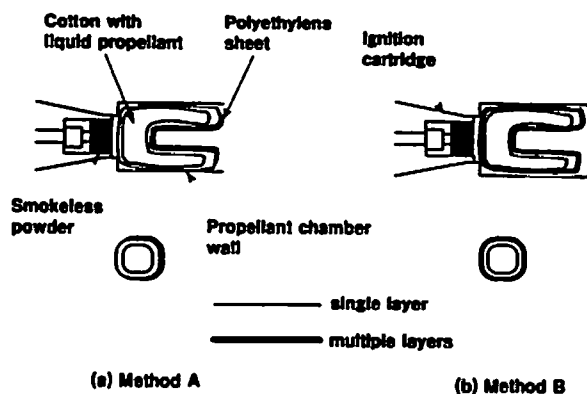


Fig. 6 Methods of propellant loading

film, and was placed at the end of the propellant chamber near the smokeless powder. The bag was folded several times. Fig. 6 schematically illustrates two methods of folding the bag; in the Method A, the bag is folded so that the liquid propellant is separated from the smokeless powder only by a single layer of polyethylene sheet; in the Method B, it was folded so that the propellant is wrapped by seven layers of polyethylene sheet.

Muzzle speeds were distinctly affected by the difference between the Methods A and B, and summarized in Fig. 7. In Fig. 7, the diaphragm rupture pressure was 20MPa . The number of folding was kept constant in each method. Relatively high performance and better degree of reproducibility were obtained with the Method A. A muzzle speed of 950m/s was achieved by using the liquid propellant of 35g . The

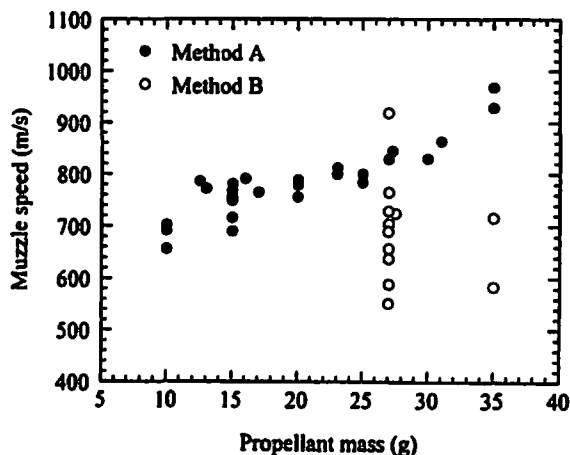


Fig. 7 Ballistic performance with two different propellant loading methods. $p_r = 20 \pm 3\text{MPa}$

scatter in the muzzle velocity was $\pm 6\%$ (for propellant mass of 15g) at most. The muzzle speed is not found to be sensitive to the variation of propellant mass. As will be shown later, the ballistic performance for a larger amount of liquid propellant can be improved by adjusting the diaphragm rupture pressure.

As seen in Fig. 7, the muzzle speed with the Method B scatters $\pm 25\%$ with liquid propellant of 27g and shows poorer degree of reproducibility. The muzzle speed is much lower in almost all cases.

Fig. 8 shows the time variations of p_1 for Methods A and B. The abscissa represents a time, t , measured from the moment of noticeable pressure rise. Δt_A and Δt_B designate time intervals from initiation of the pressure rise to a pressure drop due to expansion waves originated in diaphragm rupture in the Methods of A and B, respectively. In both cases, the pressure slowly rises to reach an almost constant value of 5.5MPa at $t = 7$ ms. In the Method A, the pressure rise due to the main combustion appears at $t = 10$ ms. However, in the Method B the pressure rise appears delayed by 11ms. When it starts increasing again at $t = 21$ ms, the pressure already decreases by about 30% ; from 5.5MPa to 4.0MPa. For this long delay time interval, the heat loss from the combustion product gas to the propellant chamber wall causes the significant pressure drop. Also the rate of pressure increase after $t = 21$ ms is lowered in the case of the Method B.

In Table 1, Δt_A , Δt_B and their scatters are com-

Table 1 Measured values of Δt_A and Δt_B defined in Fig. 8, and their scatters. Liquid propellant (LP) ; 25 to 30g

Quantity	Value
Δt_A	14.8 ± 0.7 ms
Δt_B	28.8 ± 7.8 ms

pared between the two methods. Δt_A is about the half of Δt_B . Moreover, scatter in Δt_A is about one-tenth of that of Δt_B . It is concluded from these results that the pyrolysis process is sensitive to the method of loading the liquid propellant. The ignition of the liquid propellants would be delayed if its loading is not properly done. The heat loss to the propellant chamber wall lowers the main combustion rate, resulting in the degradation of the ballistic performance.

4.3 Ballistic performance

In this section, ballistic performance out of data collected with only the Method A will be discussed. As seen in Fig. 7, keeping a diaphragm rupture pressure constant, the muzzle velocity is a weak function of the mass of the liquid propellant. Fig. 9 shows dependences of the muzzle speed on the diaphragm rupture pressure. It is found that the muzzle speed sharply increases with increasing the rupture pressure.

This tendency is well interpreted with in-bore projectile acceleration profiles obtained by the VISAR (Fig. 10) and with the time variations of p_1 (Fig. 11), both of which were measured with different

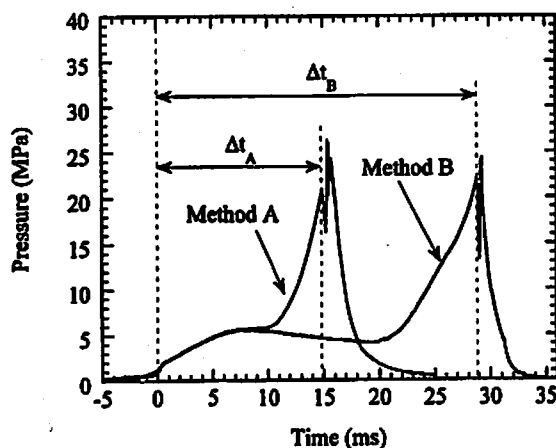


Fig. 8 Typical histories of p_1 with Methods A and B. LP ; $p_r = 20 \pm 3$ MPa

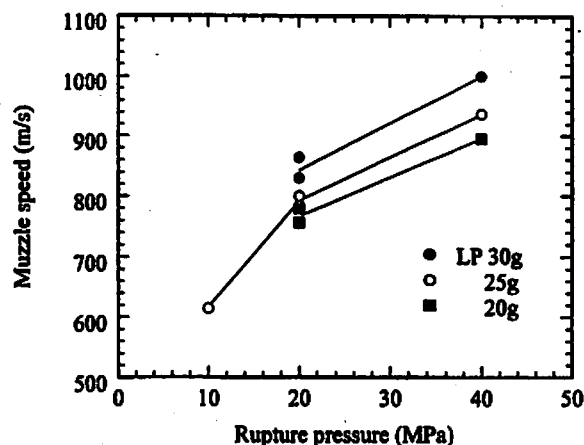


Fig. 9 Muzzle speed as a function of diaphragm rupture pressure, p_r

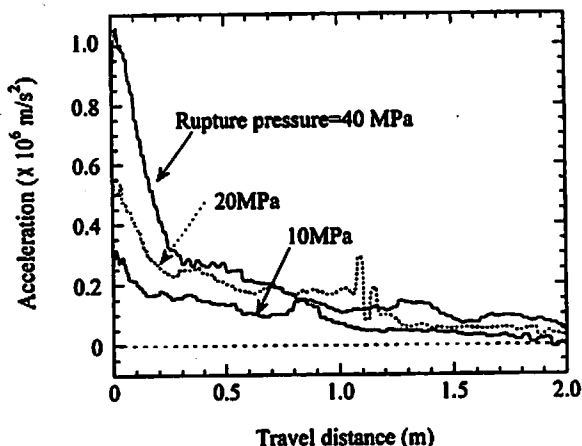


Fig. 10 In-bore projectile acceleration profiles with different diaphragm rupture pressures. LP ; 25g

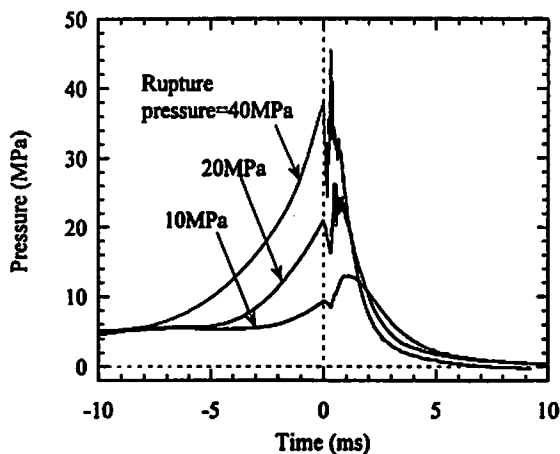


Fig. 11 Propellant chamber pressure (p_1) histories measured with different diaphragm rupture pressures. LP ; 25g. $t = 0$ corresponds to the arrival of an expansion wave generated by diaphragm rupture

diaphragm rupture pressures. In Fig. 10, the acceleration of the projectile is estimated by differentiating the time variation of the measured projectile in-tube velocity. The projectile travel distance is calculated by integrating the in-tube velocity profile. In Fig. 10, the integration of this acceleration-distance profile scales with a projectile kinetic energy gain. The acceleration is done mainly near the diaphragm - in the first 20% of the total length of the launch tube. The amount of energy input in this region is determined mainly by the diaphragm rupture pressure. In Fig. 11, at the lowest rupture pressure, the propellant chamber pressure does not reach such high values

as of the others. In this case, the diaphragm is ruptured at the earlier stage of the liquid propellant combustion, thereby the combustion is quenched. For the rupture pressure of 20MPa, the pressure once decreased due to the diaphragm rupture and recovered to some extent. For the rupture pressure of 40MPa, the combustion is almost completed so that, filtering out high-frequency oscillatory components, the propellant chamber pressure reaches its maximum when the diaphragm is ruptured. In general, the rate of pressure increase generated by liquid propellant combustion is modest²¹. The combustion tends to be readily quenched by expansion waves caused by the diaphragm rupture. It follows from these results that because of the modest burning rate the peak value of the projectile acceleration is determined mainly by the diaphragm rupture pressure. When the rupture pressure is high, the energy gain through the projectile acceleration is much enhanced, and hence increasing the ballistic performance.

5. Conclusions

Basic characteristics of the liquid propellant, LP1846, are experimentally investigated. The method of the propellant loading is important for achieving a reproducible ballistic performance. Since the propellant combustion rate is modest, the peak acceleration strongly depends on the diaphragm rupture pressure. Under the conditions of the present study, the muzzle speed increased with the rupture pressure. This tendency is not necessarily favorable for attaining a high piezometric efficiency. Further parametric studies are necessary to identify operation regimes in which the ballistic performance of the liquid propellant becomes preferable to that of solid propellant.

Acknowledgment

The authors would like to express their gratitude to Professor E. Zaretsky, Ben-Gurion University of the Negev, Israel, for his assistance in preparing for the VISAR measurement. The authors thank for assistances dedicated by Dr. O. Onodera, Messrs H. Ojima, H. Ogawa, M. Adachi, K. Takahashi, N. Ito and M. Kato of Institute of Fluid Science. The authors acknowledge Asahi Chemical Industry Co., Ltd., Oita, Japan, for its supplying with liquid propellant.

References

- 1) A. Sasoh, Y. Hamate and K. Takayama, AIAA paper 98-3446 (1998) .

- 2) G. Klingenberg, J. D. Knapton, W. F. Morrison and G. P. Wren, "Liquid Propellant Gun Technology", Progress in Astronautics and Aeronautics, Vol. 175 (1997) AIAA
- 3) A. Shibata, J. Ind. Expl. Soc. Japan (in Japanese) 49, 73 (1988)
- 4) H. Bazaki, Y. Kosaka and D. Kameyama, Proc. of Annual Meeting, Ind. Expl. Soc. Japan (in Japanese), P. 1 (1988)
- 5) T. Kuwahara and I. Nakagawa, Proc. Annual Meeting, Ind. Expl. Soc. Japan (in Japanese), P. 68 (1989)
- 6) T. Kishida, T. Tachibana and Y. Kosaka, J. Ind. Expl. Soc. Japan (in Japanese) 53, 290 (1992)
- 7) D. Meinhardt, G. Brewster, S. Chricofferson and E. J. Wucherer, AIAA paper 98-4006 (1998)
- 8) M. E. Kounalakis and G. M. Faeth, Combust. and Flame 74, 179 (1988)
- 9) S. Ohba, "Study on Ballistic Range Performance Using a Liquid Propellant", Master thesis (in Japanese), Tohoku University, Japan, March 1999.
- 10) L. M. Barker and R. E. Hollenbach, J. Appl. Phys. 43, 4669 (1972)
- 11) D. E. Munson and R. P. May, AIAA J. 14, 235 (1976)

液体発射薬のバリステックレンジ実験への応用に関する研究

佐宗章弘*, 大庭真治**, 高山和喜*

HANを基材とした一液性液体発射薬LP1846を用いて、バリステックレンジ実験を行った。実験は、発射管内径25mmの一段銃を用いた。10～35gの液体発射薬をバルク装填し、発射管出口速度1.0km/sを得た。火薬室圧力、飛行体の管内速度履歴を測定した。液体発射薬の燃焼は、熱分解に起因する遅れ時間を伴う。再現性の良い性能を得るためには、装薬方法に注意を払う必要があることが分かった。更に、発射管出口速度は、火薬室と発射管の間におかれた隔膜の破断圧に強く依存することが確かめられた。

(*東北大学流体科学研究所衝撃波研究センター 〒980-8577 仙台市青葉区片平2-1-1)

**東北大学大学院工学研究科 航空宇宙工学専攻)